

Report No.
UCB/SEMM-2011/07

Structural Engineering
Mechanics and Materials

**Analysis of a class of high-order local
absorbing boundary conditions**

By

Koki Sagiya and Sanjay Govindjee

June 2011

Department of Civil and Environmental Engineering
University of California, Berkeley

Analysis of a class of high-order local absorbing boundary conditions

Koki Sagiyama^a, Sanjay Govindjee^{a,*}

*^aStructural Engineering, Mechanics and Materials
Department of Civil Engineering
University of California, Berkeley
Berkeley, CA 94720-1710, USA*

Abstract

Radiation or absorbing boundary conditions are a requisite element of many computational wave propagation problems. In this work we examine the high-order absorbing boundary conditions with auxiliary functions first developed by Givoli and Neta and later modified by Hagstrom and Warburton. Such boundary conditions have been proven to provide excellent behavior in the time harmonic setting yet are formulated in a manner that makes them also directly applicable to time domain computations. In this work we look at two issues that have not received a lot of study: (1) uniqueness of the solution and (2) the eigen-structure of the overall problem. Both issues are intimately tied to the practical performance of such boundary conditions. In particular we show from the eigen-structure that these higher-order absorbing boundary conditions can not in general provide better long-time accuracy than lower-order absorbing boundary conditions. Second we conjecture that the (possible) non-uniqueness of solutions to the overall problem can lead to the observed long-time instabilities seen in the literature.

Keywords: absorbing boundary conditions, radiation boundary conditions, high-order local absorbing boundary conditions

*Corresponding author

Email addresses: `sagiyama999@berkeley.edu` (Koki Sagiyama), `s_g@berkeley.edu` (Sanjay Govindjee)

1. Introduction

Analysis of wave propagation in an unbounded domain has been of interest in many fields including for example geotechnical engineering and electromechanics. Due to unboundedness, this type of problem does not allow direct application of standard numerical solvers such as finite element methods which require a finite domain. Thus one needs a completely new methodology or a mapping of the problem to a finite domain. Within the class of mapped methods, a natural one is to truncate the unbounded domain, introduce non-physical boundaries around the resulting bounded domain, and then apply appropriate boundary conditions on the new boundaries to mimic the effect of the original unboundedness. These boundary conditions are called absorbing or radiation boundary conditions and they have been important topics in mathematics and engineering; see e.g. [1] or [2] for recent reviews. Among several classes of absorbing boundary conditions, we focus our attention on the Hagstrom and Warburton [3] high-order local absorbing boundary conditions using auxiliary functions as first introduced by Givoli and Neta in [4]. Additionally, we will examine the so-called *complete radiation boundary conditions* also developed by Hagstrom and Warburton [5].

The Givoli and Neta [4] conditions are a re-writing of the classic high-order Higdon conditions [6] from a high-order differential operator into a recursive system of first-order differential operators using auxiliary variables. Mathematically nothing is changed but it greatly facilitates numerical computations due to the lowering of the differential order; this later point is strongly aided by Givoli and Neta's transformation of the normal boundary derivatives into a second-order form using only tangential boundary derivatives. It should be noted that the conversion to second-order form involves a modeling choice and is non-unique. Hagstrom and Warburton [3] modified the recursion form of [4] in a manner that squares the reflection coefficient of [4] (when analyzing time-harmonic plane waves), symmetrizes the formulation, and improves its overall behavior. However it should be noted that example computations [3, Figs. 2 and 3] show a troubling instability in time, viz., errors growing in time. Further, in a certain sense, low-order methods are seen to perform better than high-order methods – essentially contradicting the error analysis in the plane wave setting. Analytical work on stability shows that the continuous form of the Givoli and Neta conditions and the Hagstrom and Warbuton conditions to be stable [7, 8] but numerical computations belie this point; in addition to the perviously cited examples, see

also [7, Fig. 8], [9, Fig. 2], and [10, Figs. 7 and 8]. Similar remarks, vis-a-vis long time error, also pertain to the complete radiation boundary conditions [5].

In this paper we look at the issues of stability and accuracy for the two Hagstrom and Warbuton forms of the local high-order absorbing boundary condition. It is our intent to explain the undesired numerical behavior which appears when performing actual computations. In Section 2, we show analytically that solutions to problems with these types of boundary conditions are not unique unless special care is taken with respect to the boundary conditions and that the eigenvalues for such systems are nested; that is, by increasing the order of the absorbing boundary conditions, one only adds, and never removes, eigenvalues and eigenmodes. This latter issue is crucial for the case where the accuracy of the solution is governed by the rate of dissipation which is determined by the least negative eigenvalue in the system (instead of the reflection coefficients). A problem of pulse excitation belongs to this category. In Section 3, we introduce a second order formulation of the complete radiation boundary conditions which also includes as a special case the second order formulations proposed in [4, 3]. Finally in Section 4, we numerically solve a two dimensional waveguide problem with a pulse excitation using our second order formulations. We observe smaller rates of dissipation for the higher order formulations after the pulse leaves the domain, which reflects the issue of the nesting of eigenvalues discussed in Section 2. Also, while complete radiation boundary conditions give stable solutions for a long time, we observe that the use of the conditions in [3] leads to polynomial growth of the error. The sources of this instability have not been known, but we believe that we have made an improvement on this issue through close observations of our example – viz. that they are associated with a non-uniqueness issue. Section 5 concludes.

2. Analysis

2.1. Absorbing boundary conditions: Hagstrom and Warburton [3]

We start by considering the high-order absorbing boundary conditions for a scalar wave problem in d -dimensional space proposed by Hagstrom and Warburton in [3]. Let $u(x, \mathbf{y}, t)$ ($\mathbf{y} \in \mathcal{R}^{d-1}$) satisfy the scalar wave equation on a domain \mathcal{D} ,

$$\nabla^2 u = \frac{1}{c^2} \ddot{u} \quad \text{on } \mathcal{D}, \quad (1)$$

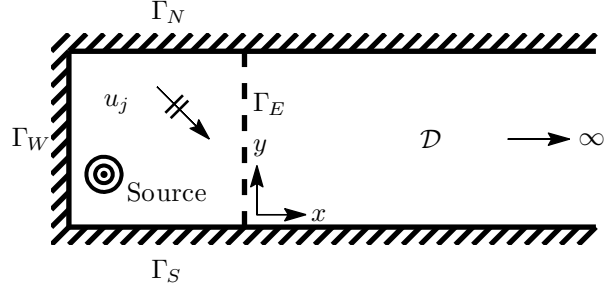


Figure 1: Example waveguide problem. The hatches represent Dirichlet boundary conditions. The waveguide is originally unbounded in the positive x direction, but this unboundedness is replaced by the absorbing boundary on Γ_E .

with sources and boundary conditions in $x < 0$. We assume that the domain \mathcal{D} is unbounded and homogeneous in $x > 0$. We then truncate it at $x = 0$ and apply absorbing boundary conditions on the resulting artificial boundary. Figure 1 shows an example waveguide problem. In this example, Dirichlet boundary conditions are applied on Γ_W , Γ_N , and Γ_S , and absorbing boundary conditions are applied on Γ_E , replacing the unbounded domain, $x > 0$. We are interested in the error due to this substitution.

The high-order absorbing boundary conditions proposed in [3] is given by,

$$\left(\frac{\cos \phi_0}{c} \frac{\partial}{\partial t} + \frac{\partial}{\partial x} \right) u_0 = \frac{\partial u_1}{\partial t}, \quad (2a)$$

$$\left(\frac{\cos \phi_j}{c} \frac{\partial}{\partial t} + \frac{\partial}{\partial x} \right) u_j = \left(\frac{\cos \bar{\phi}_j}{c} \frac{\partial}{\partial t} - \frac{\partial}{\partial x} \right) u_{j+1}, \quad (2b)$$

$$u_{p+1} = 0, \quad (2c)$$

for $j = 1, \dots, p$. In (2a) and (2b), $u_0(x, \mathbf{y}, t)$ represents $u(x, \mathbf{y}, t)$, $u_j(x, \mathbf{y}, t)$ are auxiliary functions, and ϕ_j and $\bar{\phi}_j$ are parameters chosen in $[0, \pi/2)$. p is called the order of the absorbing boundary conditions, and we expect that the error due to truncation decreases as one increases the order. In addition to (2), we require u_j to satisfy the wave equation, or,

$$\nabla^2 u_j = \frac{1}{c^2} \ddot{u}_j \quad \text{on } \mathcal{D}. \quad (3)$$

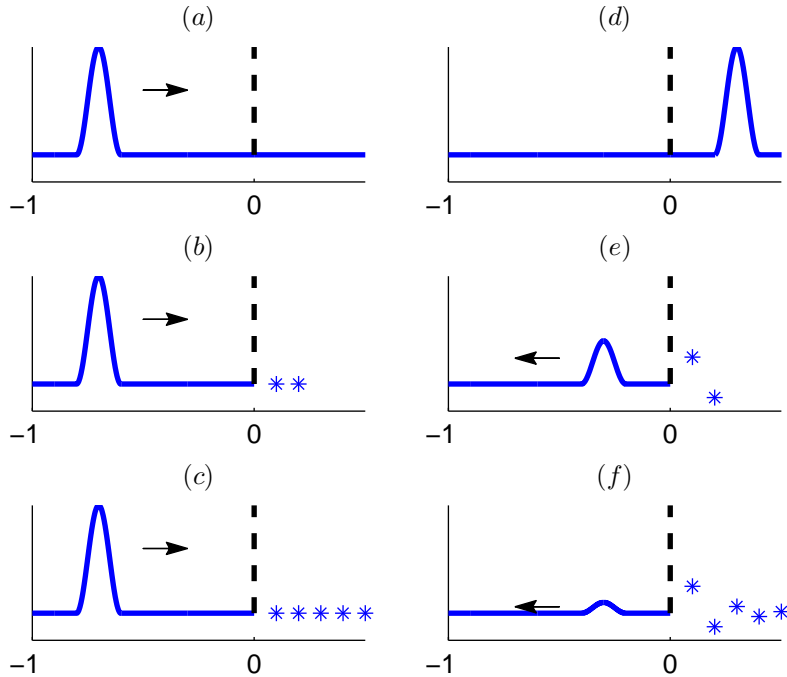


Figure 2: Schematic pictures of a one-dimensional scalar wave problem with pulse excitation at $x = -1$ and high-order absorbing boundary conditions at $x = 0$. (a), (b), and (c) show the displacement fields before the pulse reaches the boundary for the original unbounded problem and problems with absorbing boundary conditions of two different orders $p_1 = 2$ and $p_2 = 5$. The '*' represents each auxiliary function. (d) shows the exact solution one would observe if the domain was unbounded right after the pulse left the domain. (e) and (f) show the reflections and the displacement fields for auxiliary functions at the same time as (d) for the two different orders.

We are to impose (2) at $x = 0$ to represent the boundary derivatives on the artificial boundary.

2.1.1. Uniqueness

We assume here that a set of solutions u_j exists for the system characterized by (1), (2), (3), and boundary conditions for u on $x < 0$, for each given order p , and that $u_p(x, \mathbf{y}, t)$ is not identically zero. We now consider two problems, one of order p_1 and one of higher order $p_2 > p_1$. To simplify the discussion, we assume that for these two problems the same sets of parameters ϕ_j and $\bar{\phi}_j$ are chosen for $j = 0, 1, \dots, p_1$. By assumption, each problem possesses a solution denoted by $u_j^{(1)}$ and $u_j^{(2)}$ with $u_{p_1}^{(1)} \neq 0$ and $u_{p_2}^{(2)} \neq 0$,

respectively. One then realizes that the following functions give another set of solutions to the problem of order p_2 :

$$\begin{aligned} u_j &= u_j^{(1)} & j &= 0, 1, \dots, p_1, \\ u_j &= 0 & j &= p_1+1, \dots, p_2. \end{aligned} \tag{4}$$

Thus the solution to the problem is not unique unless appropriate boundary conditions are specified for u_j ($j = 1, \dots, p$). In general, such conditions can not be known without first knowing the true solution u_0 .

2.1.2. Nested Eigenvalues

For these two systems of orders p_1 and p_2 , one also observes that the latter possesses all the eigenvalues and eigenmodes present in the former. Here we refer to λ ($Re(\lambda) \leq 0$) as the eigenvalues and \bar{u}_j as the eigenmodes in the decomposition $u_j(x, \mathbf{y}, t) = \bar{u}_j(x, \mathbf{y})e^{\lambda t}$. This nesting can be readily shown by setting,

$$\begin{aligned} \bar{u}_j^{(2)} &= \bar{u}_j^{(1)}, & j &= 0, 1, \dots, p_1, \\ \bar{u}_j^{(2)} &= 0, & j &= p_1+1, \dots, p_2, \end{aligned}$$

where $\bar{u}_j^{(1)}$ and $\bar{u}_j^{(2)}$ are eigenmodes for systems of orders p_1 and p_2 . Denoting by $\mathcal{S}^{(1)}$ and $\mathcal{S}^{(2)}$ the sets of eigenvalues to the problems of order p_1 and p_2 , respectively, one can say $\sup\{\mathcal{S}^{(1)}\} \leq \sup\{\mathcal{S}^{(2)}\}$. This implies that the least negative eigenvalue in the system of order p_2 can be no smaller than that in the system of order p_1 . The problem caused by these nested eigenvalues is explained through a simple example. Suppose a one-dimensional half-space problem with pulse excitation at $x = -1$. The domain is unbounded in the positive x direction, but we truncate it at $x = 0$ and apply high-order absorbing boundary conditions, say of orders $p_1 = 2$ and $p_2 = 5$. We compare the exact solution of the original unbounded problem with solutions with these absorbing boundary conditions. Before the pulse reaches the boundary, the solutions should all look the same as shown in Figures 2(a), 2(b), and 2(c). After the pulse hits the boundary, however, the exact solution should leave nothing in the domain $-1 \leq x \leq 0$, while the absorbing boundaries cause reflections which go back and forth between the two boundaries as they, *hopefully*, decay. The auxiliary variables are also excited. See Figures 2(d), 2(e), and 2(f) for schematic pictures. The accuracy of the solutions by absorbing boundary conditions is then eventually determined merely by the rates of

dissipation in this phase of free vibration, which is governed by the least negative eigenvalues in the systems. Therefore, the analysis above implies that a system with higher order boundary conditions can not converges to the exact solution faster by nature, since $\sup\{\mathcal{S}^{(1)}\} \leq \sup\{\mathcal{S}^{(2)}\} \leq 0$. We also note that, if the parameters ϕ_j and $\bar{\phi}_j$ for $j = 0, 1, \dots, p_1$ are chosen independently for the two systems of orders p_1 and p_2 , the eigenvalues of the two are not nested any more in general. However, it can be readily shown that the least negative eigenvalue of the latter with optimal choices of parameters can be no smaller than that of the former.

The observation above does not necessarily guarantee the poorer behavior of higher order formulations in problems for which rates of dissipation are concerned, since, due to the lack of uniqueness of the solution, physically meaningful problems require additional restrictions and these restrictions can prevent slowly dissipating modes of the higher order conditions from being excited. Indeed in the duct problem with pulse input in [5], which was numerically solved using the first order form of the scalar wave equation, slower rates of dissipation for higher order formulations are not readily observable in the plots presented. However, in the waveguide problem presented in Section 4 using the second order formulation derived in Section 3, we do observe the poorer dissipation rates for larger values of p .

2.2. Complete radiation boundary conditions

We next consider the complete radiation boundary conditions proposed in [5], which are given by,

$$\left(\frac{\cos \phi_j}{c} \frac{\partial}{\partial t} + \frac{\partial}{\partial x} + \frac{1}{cT} \frac{\sin^2 \phi_j}{\cos \phi_j} \right) u_j =$$

$$\left(\frac{\cos \bar{\phi}_j}{c} \frac{\partial}{\partial t} - \frac{\partial}{\partial x} + \frac{1}{cT} \frac{\sin^2 \bar{\phi}_j}{\cos \bar{\phi}_j} \right) u_{j+1}, \quad (5a)$$

$$u_{p+1} = 0, \quad (5b)$$

where ϕ_j and $\bar{\phi}_j$ are defined as in (2) and T is an additional parameter with dimensions of time. We also require u_j to satisfy (3). Assuming again that the system given by (1), (5), (3) with sources and boundary conditions for u in $x < 0$ possesses a solution, one can show in the same way that the issues of non-uniqueness of the solution and nested eigenvalues are also present in this formulation.

3. Second order formulation

To numerically solve the problem introduced in Section 2 with the finite element method, for instance, it is computationally more efficient if the auxiliary functions u_j live only on the boundary. However, in that case, the normal derivatives on the boundary $x = 0$ appearing in (2) and (5) can not be represented. To overcome this problem, we derive a family of second order formulations, which includes the second order formulation in [3] as a special case.

We first realize that one can rewrite the system of equations (5) in a matrix form as,

$$\mathbf{M}_1 \mathbf{U}_{,x} = \frac{1}{c} \mathbf{M}_2 \dot{\mathbf{U}} + \frac{1}{cT} \mathbf{M}_3 \mathbf{U}, \quad (6)$$

where $\mathbf{U} = [u_0, u_1, \dots, u_p]^T$ and \mathbf{M}_1 , \mathbf{M}_2 , and \mathbf{M}_3 are $(p+1) \times (p+1)$ matrices of coefficients in (5). \mathbf{M}_1 being invertible, we have,

$$\mathbf{U}_{,x} = \frac{1}{c} \mathbf{M}_t \dot{\mathbf{U}} + \frac{1}{cT} \mathbf{M}_0 \mathbf{U}, \quad (7)$$

where $\mathbf{M}_t = \mathbf{M}_1^{-1} \mathbf{M}_2$ and $\mathbf{M}_0 = \mathbf{M}_1^{-1} \mathbf{M}_3$. Here, \mathbf{M}_t and \mathbf{M}_0 as well as \mathbf{M}_1 , \mathbf{M}_2 , and \mathbf{M}_3 are upper-triangular matrices. Note that the first row of equation (7) enables one to replace the normal boundary derivative of u_0 on $x = 0$ merely with time derivatives of u_j , which helps in numerical implementations. Now, taking another x -derivative of equation (7) and using (7) again to eliminate arising x -derivative terms on the R.H.S., we obtain a necessary condition to the set of equations (7), or,

$$\mathbf{U}_{,xx} = \frac{1}{c^2} \mathbf{M}_t^2 \ddot{\mathbf{U}} + \frac{1}{c^2 T} (\mathbf{M}_t \mathbf{M}_0 + \mathbf{M}_0 \mathbf{M}_t) \dot{\mathbf{U}} + \frac{1}{c^2 T^2} \mathbf{M}_0^2 \mathbf{U}. \quad (8)$$

Since we force each $u_j(x, \mathbf{y}, t)$ to satisfy the wave equation, we can rewrite (3) as,

$$\mathbf{U}_{,xx} + \nabla_{\tan}^2 \mathbf{U} = \frac{1}{c^2} \ddot{\mathbf{U}},$$

where $\nabla_{\tan}^2 \mathbf{U}$ represents the Laplacian of \mathbf{U} on the boundary. With this we can eliminate $\mathbf{U}_{,xx}$ in (8) and obtain,

$$T^2 (\mathbf{M}_t^2 - \mathbf{I}) \ddot{\mathbf{U}} + T (\mathbf{M}_t \mathbf{M}_0 + \mathbf{M}_0 \mathbf{M}_t) \dot{\mathbf{U}} + \mathbf{M}_0^2 \mathbf{U} + c^2 T^2 \nabla_{\tan}^2 \mathbf{U} = \mathbf{0},$$

which only involves time derivatives and spatial derivatives in \mathbf{y} -directions, and so allows discretization on $x = 0$. Finally, one can multiply this equation by any $(p + 1) \times (p + 1)$ invertible matrix, say \mathbf{D} , and obtain,

$$T^2 \mathbf{D} (\mathbf{M}_t^2 - \mathbf{I}) \ddot{\mathbf{U}} + T \mathbf{D} (\mathbf{M}_t \mathbf{M}_0 + \mathbf{M}_0 \mathbf{M}_t) \dot{\mathbf{U}} + \mathbf{D} \mathbf{M}_0^2 \mathbf{U} + c^2 T^2 \mathbf{D} \nabla_{\tan}^2 \mathbf{U} = \mathbf{0}. \quad (9)$$

We then replace equations (5) with (9). Note that a similar analysis as given in Section 2 shows that the overall problem remains, in general, non-unique and the eigenvalues nested. Regarding the non-uniqueness of the solution, our new system also possesses more solutions since it is the necessary condition of the original. We also note that, by merely discretizing p rows out of $p + 1$ of (9) along the boundary, we obtain a sufficient number of equations for determining the p auxiliary functions, and we are to ignore one row in (9). In the waveguide example given in Section 4, we realize that elimination of the last row happens to exclude the solutions of the form given in (4) upon discretization, and we can indeed obtain a unique solution in the case of the complete radiation boundary conditions.

Finally, we observe that the numerical solution is very sensitive to the choice of \mathbf{D} , even though it is not in the continuous setting. A choice of \mathbf{D} which gives a satisfactory solution was found, motivated by the coefficients in the second order formulation in [3], by,

$$\mathbf{D} = \begin{bmatrix} a_1 & a_0 + a_1 & a_0 & 0 & \dots & 0 \\ 0 & a_2 & a_1 + a_2 & a_1 & \dots & 0 \\ 0 & 0 & a_3 & a_2 + a_3 & \dots & 0 \\ 0 & 0 & 0 & a_4 & \dots & 0 \\ \vdots & \vdots & \vdots & \vdots & \ddots & \vdots \\ 0 & 0 & 0 & 0 & \dots & 1 \end{bmatrix}. \quad (10)$$

Also note that by setting $\mathbf{M}_1(1, 2) = 0$, $\mathbf{M}_2(1, 2) = 1$, and $\mathbf{M}_3 = \mathbf{0}$, or equivalently $\mathbf{M}_0 = \mathbf{0}$, and selecting \mathbf{D} as,

$$\mathbf{D} = \begin{bmatrix} 2a_1 & 1 & 1 & 0 & \dots & 0 \\ 0 & a_2 & a_1 + a_2 & a_1 & \dots & 0 \\ 0 & 0 & a_3 & a_2 + a_3 & \dots & 0 \\ 0 & 0 & 0 & a_4 & \dots & 0 \\ \vdots & \vdots & \vdots & \vdots & \ddots & \vdots \\ 0 & 0 & 0 & 0 & \dots & 1 \end{bmatrix}, \quad (11)$$

we recover the second order formulation of [3]; in (10) and (11) we have introduced $a_j = \cos \phi_j = \cos \bar{\phi}_j$.

4. Numerical examples

We now solve a two-dimensional waveguide problem for the scalar wave equation to demonstrate the behavior of the high-order absorbing boundary conditions using the second order formulation derived in Section 3; see Figure 3 for geometry and notation. The depth of the waveguide is 1 unit and the speed of the wave is $c = 1$ unit. We apply a pulse excitation,

$$u\left(-\frac{1}{2}, y\right) = \begin{cases} \cos(\pi y)(1 - \cos 4\pi t), & 0 \leq t \leq 1/2 \\ 0, & 1/2 < t \end{cases} \quad (12)$$

on Γ_W and homogeneous Neumann boundary conditions on Γ_N and Γ_S . We truncate this infinitely long waveguide at $x = 0$ and apply the different types of absorbing boundary conditions mentioned earlier, where we consistently set $\phi_j = \bar{\phi}_j$ and choose their values according to the Gauss quadrature nodes in $[0, \pi/2)$ motivated by [5]. We also set $T = 1$. We use an implicit 2nd order accurate Newmark scheme ($\beta = 1/4$, $\gamma = 1/2$) for time-stepping with $\Delta t = 0.01$ and a finite element method with 16×8 square bi-cubic elements in Ω and 16 cubic elements for each u_j along Γ_E . The discretization along the boundary requires boundary conditions for each auxiliary function $\partial u_j / \partial y$ at both ends of Γ_E . In this example, we assume that the same boundary conditions as for u_0 on Γ_N and Γ_S can be applied; i.e. we set $\partial u_j / \partial y = 0$ on $\Gamma_N \cap \Gamma_E$ and $\Gamma_S \cap \Gamma_E$ as in [7].

We first apply the second order formulation introduced in [3], that is, we set $\mathbf{M}_1(1, 2) = 0$, $\mathbf{M}_2(1, 2) = 1$, $\mathbf{M}_0 = \mathbf{0}$ and choose \mathbf{D} given in (11). Figure 4 shows the plots of $\log \|u_0\|_2$ on Γ_E against $\log t$. We observe that a polynomial growth, or a linear growth in log-log scale, of the l_2 -norm becomes evident after a long time. To explain this instability, we consider the homogeneous part of the equations of motion obtained by discretizing (1) and (9) along with the first row of (7) in space and applying the boundary condition (12) on Γ_W , or,

$$\mathbf{M}\ddot{\mathbf{u}} + \mathbf{C}\dot{\mathbf{u}} + \mathbf{K}\mathbf{u} = \mathbf{0}, \quad (13)$$

where \mathbf{M} , \mathbf{C} , and \mathbf{K} are mass, damping, and stiffness matrices, and $\mathbf{u} = [\mathbf{u}_0, \mathbf{u}_1, \dots, \mathbf{u}_p]^T$ is a set of nodal displacements including those for auxiliary

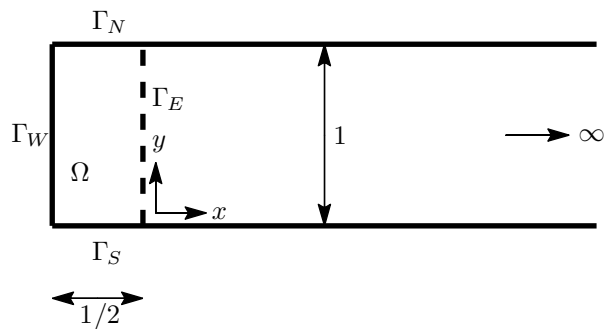


Figure 3: Waveguide setup.

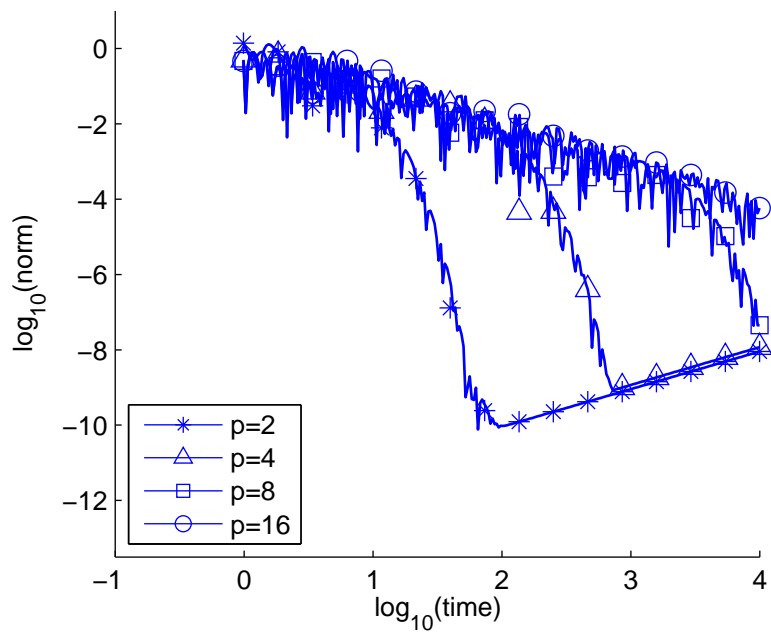


Figure 4: Plots of $\log_{10} \|u_0\|_2$ on Γ_E versus $\log_{10} t$ for select orders for the modified formulation. [3]

functions. We then set $\mathbf{u}(t) = \bar{\mathbf{u}}e^{\lambda t}$ with $\bar{\mathbf{u}} = [\bar{\mathbf{u}}_0, \bar{\mathbf{u}}_1, \dots, \bar{\mathbf{u}}_p]^T$ in the semi-discrete system (13), and obtain,

$$(\lambda^2 \mathbf{M} + \lambda \mathbf{C} + \mathbf{K}) \bar{\mathbf{u}} = \mathbf{0}. \quad (14)$$

Here, since the stiffness matrix \mathbf{K} in (14) stems only from the discretization of the second order spatial derivatives in (1) and (9), a vector $\bar{\mathbf{u}}$ with,

$$\begin{aligned} \bar{\mathbf{u}}_k &= \text{non-zero constant} && \text{for one } k \in \{1, \dots, p\}, \\ \bar{\mathbf{u}}_j &= 0 && j = 0, 1, \dots, k-1, k+1, \dots, p, \end{aligned}$$

satisfies $\mathbf{K}\bar{\mathbf{u}} = \mathbf{0}$ and so is an eigenvector corresponding to eigenvalue $\lambda = 0$ according to (14). Indeed, we observe $2p$ zero-eigenvalues when we consider the equivalent first order system to equation (13),

$$\left[\begin{array}{c|c} \mathbf{I} & \mathbf{0} \\ \hline \mathbf{0} & \mathbf{M} \end{array} \right] \begin{bmatrix} \dot{\mathbf{u}} \\ \mathbf{v} \end{bmatrix} = \left[\begin{array}{c|c} \mathbf{0} & \mathbf{I} \\ \hline -\mathbf{K} & -\mathbf{C} \end{array} \right] \begin{bmatrix} \mathbf{u} \\ \mathbf{v} \end{bmatrix}, \quad (15)$$

where $\mathbf{v} = \dot{\mathbf{u}}$. The coefficient matrix on the L.H.S. being invertible, we can rewrite (15) as,

$$\dot{\tilde{\mathbf{u}}} = \mathbf{A}\tilde{\mathbf{u}}, \quad (16)$$

where $\tilde{\mathbf{u}} = [\mathbf{u}, \mathbf{v}]^T$. \mathbf{A} can be written in Jordan canonical form with some invertible matrix \mathbf{W} as,

$$\mathbf{A} = \mathbf{W}\mathbf{\Lambda}\mathbf{W}^{-1},$$

where

$$\mathbf{\Lambda} = \begin{bmatrix} \mathbf{\Lambda}_1 & \mathbf{0} & \dots & \mathbf{0} \\ \mathbf{0} & \mathbf{\Lambda}_2 & \dots & \mathbf{0} \\ \vdots & \vdots & \ddots & \vdots \\ \mathbf{0} & \mathbf{0} & \dots & \mathbf{\Lambda}_s \end{bmatrix}, \quad \text{and,} \quad \mathbf{\Lambda}_k = \begin{bmatrix} \lambda_k & 1 & \dots & 0 & 0 \\ 0 & \lambda_k & \dots & 0 & 0 \\ \vdots & \vdots & \ddots & \vdots & \vdots \\ 0 & 0 & \dots & \lambda_k & 1 \\ 0 & 0 & \dots & 0 & \lambda_k \end{bmatrix}_{N_k \times N_k}. \quad (17)$$

In equation (17), s is the number of distinct eigenvalues of \mathbf{A} , λ_k is the k -th eigenvalue, and N_k is the number of repetition of λ_k . We now rewrite (16) as,

$$\dot{\hat{\mathbf{u}}} = \mathbf{\Lambda}\hat{\mathbf{u}}, \quad (18)$$

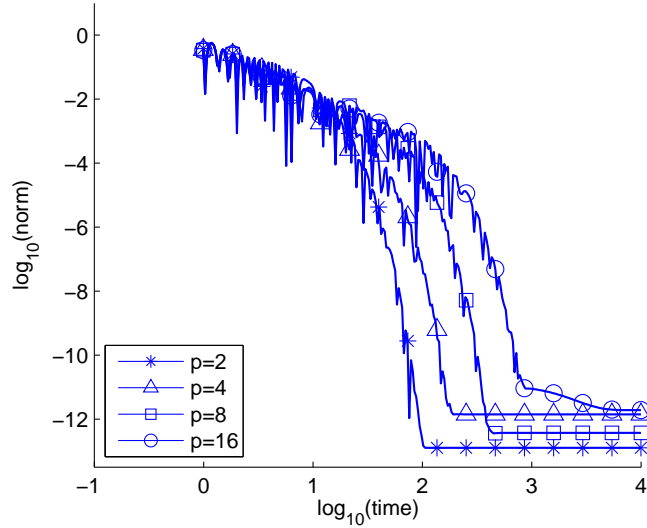


Figure 5: Plots of $\log_{10} \|u_0\|_2$ on Γ_E versus $\log_{10} t$ for select orders for the complete radiation boundary conditions.

where $\hat{\mathbf{u}} = \mathbf{W}^{-1}\bar{\mathbf{u}}$.

Here we can arbitrarily set $\lambda_1 = 0$ so that $\mathbf{\Lambda}_1$ is a $2p \times 2p$ square matrix of the form given in (17) with all diagonal elements zero. In this case, we can solve the first $2p$ rows of (18) explicitly, starting from the $2p$ -th row towards the first, as,

$$\begin{aligned}
 \dot{\hat{u}}_{2p} = 0 &\Rightarrow \hat{u}_{2p} = c_0, \\
 \dot{\hat{u}}_{2p-1} = c_0 &\Rightarrow \hat{u}_{2p-1} = c_0 t + c_1, \\
 \dot{\hat{u}}_{2p-2} = c_0 t + c_1 &\Rightarrow \hat{u}_{2p-2} = \frac{1}{2} c_0 t^2 + c_1 t + c_2, \\
 &\vdots
 \end{aligned}$$

where \hat{u}_k is the k -th element of the transformed nodal displacement vector $\hat{\mathbf{u}}$ and c_0, c_1, \dots are constants. These modes, growing in time, are excited due to numerical errors. Indeed, the plots of $\|u_0\|_2$ for $p = 2$ and $p = 4$ in Figure 4 are almost straight after a long time, and if we linearly extend these lines we realize that the intersections with the vertical line $\log_{10} t = -2 = \log_{10} \Delta t$ are of order 10^{-14} , which is a reasonable value for round-off errors.

These instabilities are not observed when we use the complete radia-

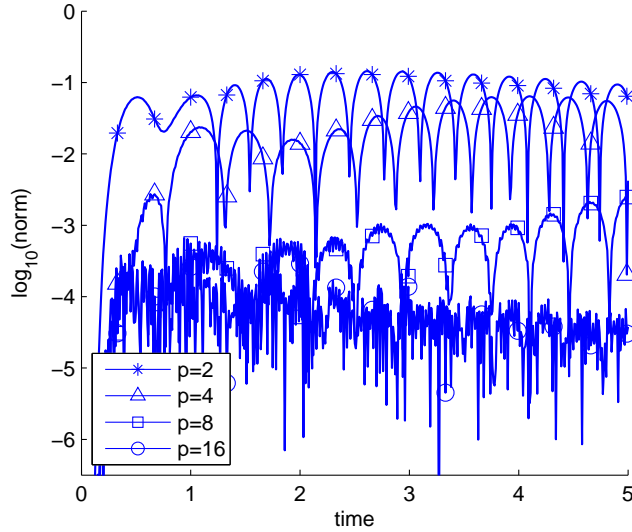


Figure 6: Plots of $\log_{10} \|u_0 - u_{exact}\|_2$ on Γ_E versus t for select orders for the complete radiation boundary conditions.

tion boundary conditions in second order form with (10), for which we have $\mathbf{M}_0 \neq \mathbf{0}$ in (9), suggesting that additional contributions from the zero-order displacement term contributes to the stiffness matrix \mathbf{K} in (14) in a manner such that the above analysis on the repeated zero-eigenvalues does not hold any more. Indeed, we observe that all the numerical eigenvalues are negative and the solutions stay stable even after a long time; see Figure 5. Though the issues on instability can be resolved in this way, Figure 5 shows slower convergence of the higher order formulations which is consistent with our analysis on eigenvalues in Section 2. On the other hand, for the first short period where reflection from the boundary governs the accuracy, higher order conditions do give smaller errors as expected, as shown in Figure 6, where the exact solution, u_{exact} , was computed in an extended waveguide.

Finally, we set $\mathbf{D}(1, 2) = 0$ in the above analysis to see the sensitivity of the solutions to the choice of \mathbf{D} . This scheme almost instantly becomes unstable and shows exponential growth of the l_2 -norm of the solution computed on Γ_E . See Figure 7 for plots of $\|u_0\|_2$ versus t for select orders. We indeed observe positive numerical eigenvalues in this system.

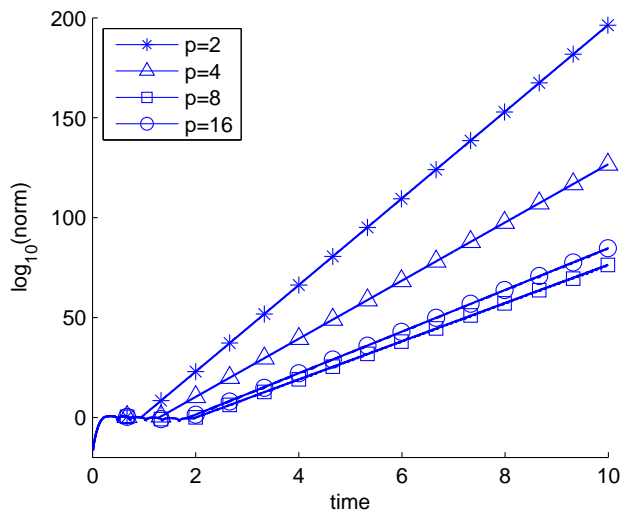


Figure 7: Plots of $\log_{10} \|u_0\|_2$ on Γ_E versus t for select orders for the complete radiation boundary conditions with inappropriate choice of \mathbf{D} .

5. Conclusion

Several issues associated with high-order absorbing boundary conditions were discussed analytically and numerically. In particular we have highlighted the fact that the introduction of auxiliary variables adds the need for additional boundary conditions which are in general unknown. In our example, we observed polynomial growth of errors with the second order formulation developed in [3] due to the presence of repeated zero-eigenvalues, and exponential error growth with the complete radiation boundary conditions in [5] with a certain choice of \mathbf{D} , while these instabilities were not observed with the complete radiation boundary conditions with an appropriate choice of \mathbf{D} . This resolution however is merely a one-off example and certainly a more robust solution is desirable. We have additionally noted, despite the proven satisfactory behavior of this class of radiation boundary conditions in terms of the reflection coefficients, that higher orders do not necessarily lead to better numerical results when dealing with problems where rates of dissipation are crucial.

6. Acknowledgment

This material is based upon work supported by the National Science Foundation under Award No. CMMI-0928785.

References

- [1] L. L. Thompson, A review of finite-element methods for time-harmonic acoustics, *Journal of the Acoustical Society of America* 119 (2006) 1315–1330.
- [2] D. Givoli, High-order local non-reflecting boundary conditions: A review, *Wave Motion* 39 (2004) 319–326.
- [3] T. Hagstrom, T. Warburton, A new auxiliary variable formulation of high-order local radiation boundary conditions: Corner compatibility conditions and extensions to first-order systems, *Wave Motion* 39 (2004) 327–338.
- [4] D. Givoli, B. Neta, High-order non-reflecting boundary scheme for time-dependent waves, *Journal of Computational Physics* 186 (2003) 24–46.
- [5] T. Hagstrom, T. Warburton, Complete radiation boundary conditions: minimizing the long time error growth of local methods, *SIAM Journal of Numerical Analysis* 47 (2009) 3678–3704.
- [6] R. Higdon, Radiation boundary conditions for dispersive waves, *SIAM Journal of Numerical Analysis* 31 (1994) 64–100.
- [7] T. Hagstrom, A. Mar-Or, D. Givoli, High-order local absorbing conditions for the wave equation: Extensions and improvements, *Journal of Computational Physics* 227 (2008) 3322–3357.
- [8] D. Baffet, D. Givoli, On the stability of the high-order Higdon absorbing boundary conditions, *Applied Numerical Mathematics* 61 (2011) 768–784.
- [9] T. Hagstrom, T. Warburton, D. Givoli, Radiation boundary conditions for time-dependent waves based on complete plane wave expansions, *Journal of Computational and Applied Mathematics* 234 (2010) 1988–1995.

- [10] D. Rabinovich, D. Givoli, J. Bielak, T. Hagstrom, A finite element scheme with a high order absorbing boundary condition for elastodynamics, *Computer Methods in Applied Mechanics and Engineering* 200 (2011) 2048–2066.